CHINESE JOURNAL OF PHYSICS VOL. 50, NO. 5 October 2012

First-Principles Molecular Orbital Calculations of the Electronic Structure and Thermoelectric Properties of Sb_2Te_3

Athorn Vora-ud,[1] Tosawat Seetawan,[1,*] Suwit Jugsujinda,[1]
Chanchana Thanachayanont,[2] and Vittaya Amornkitbamrung[3]

[1] *Thermoelectrics Research Center and Program of Physics, Faculty of Science and Technology, Sakon Nakhon Rajabhat University, Sakon Nakhon, 47000, Thailand*
[2] *National Metal and Materials Technology Center, National Science and Technology Development Agency, Pathumthani, 12120, Thailand*
[3] *Integrated Nanotechnology Research Center and Department of Physics, Faculty of Science, Khon Kaen University, Thailand*

(Received August 4, 2011; Revised January 14, 2012)

The electronic structure, electrical conductivity, and Seebeck coefficient of Sb_2Te_3 were calculated. The electronic structure was calculated by the first-principles molecular orbital method on the Hartree-Fock-Slater approximation base. The $Sb_{12}Te_{22}$ cluster model with a hexagonal base for calculating the electronic structure was designed. The calculated electronic structure shows that the crystal structure symmetry in the (100) plane, radial functions of the orbital, energy levels, partial density of states, electron occupation numbers, bond overlap population, and atomic contour maps, can induce the energy gap and Fermi level density of states values for the evaluated electrical conductivity and Seebeck coefficient.

PACS numbers: 71.15Mb, 72.15Jf, 36.20.Kd

I. INTRODUCTION

Antimony telluride (Sb_2Te_3) has excellent p-type and n-type semiconductor thermoelectric properties and superlattices [1–3], such as a large Seebeck coefficient, a high electrical conductivity, and a small thermal conductivity. The electronic structure and transport properties of Sb_2Te_3 have been measured and calculated by various techniques [4–8]. The band gap energy of Sb_2Te_3 for a single crystal, film, and bulk, are 0.15 eV [6] at 0 K, 0.29 eV [7] and 0.3 eV [8] at room temperature, respectively. The electronic structure of $Sb_2Se_xTe_{3-x}$ $(x = 1, 2)$ alloys, calculated ab initio, shows that as the phase changed from crystalline to amorphous the electric resistance increased [9]. Recently, the electronic structure of Sb_2Te_3 has been intensively investigated [4–9]. However, few studies have focused on the energy gap and Fermi level density of states to evaluate the electrical conductivity and the Seebeck coefficient.

In this paper, the crystal structure symmetry in the (100) plane, radial functions of the orbital, energy levels, partial density of states (PDOS), electron occupation numbers, bond overlap population, and atomic contour maps of Sb_2Te_3 were calculated by the molecular

*Electronic address: t_seetawan@snru.ac.th

orbital (MO) method. We evaluated the relationship for the electrical conductivity and Seebeck coefficient for the temperature range 300–700 K.

II. THEORY OF THE MOLECULAR ORBITAL, ELECTRICAL CONDUCTIVITY, AND SEEBECK COEFFICIENT

II-1. Molecular orbital calculations

In this section, we calculate the electronic structure by using a MO calculation. The MO calculation is done assuming the Hartree-Fock-Slater approximation, the linear combination of atomic orbital (LCAO) method, and the self-consistent one-electron local density theory [10–12]. The Schrödinger equation for the molecule is given by

$$\left\{-\frac{\hbar^2}{2m}\nabla^2 + V_{\text{eff}}(r)\right\}\Psi_j(r) = E_j\Psi_i(r), \tag{1}$$

where $\Psi_j(r)$ is the molecular wave function at the position r, E is the energy, $-\frac{\hbar^2}{2m}\nabla^2$ is the kinetic energy, and $V_{\text{eff}}(r)$ is the effective potential energy at the position r. The effective potential energy is

$$V_{\text{eff}}(r) = \sum -\frac{Z_N}{|r - R_N|} + \int \frac{\rho(r')}{|r - r'|}dr' + V_{XC}(r), \tag{2}$$

where Z_N is the atomic number, r is the electron position, r' is the position of the other electrons, R_N is the nucleus position, $\rho(r')$ is the electronic density at the position r', and $V_{XC}(r)$ is the exchange-correlation potential at the position r [13]. The exchange-correlation potential for Slater's Xα potential [11, 12] is given by

$$V_{XC}(r) = -3\alpha\left[\frac{3}{4\pi}\rho(r)\right]^{1/3}, \tag{3}$$

where $\rho(r)$ is the molecular electronic density at the position r and α is a constant (0.7). The molecular electronic density is given by

$$\rho(r) = \sum j\rho_j(r) = \sum j f_j\,|\Psi_j(r)|^2, \tag{4}$$

where f_j is the occupation number in the j^{th} molecular orbital. The solution of the Schrödinger equation (1) is given by

$$\Psi_j(r) = \sum (i) C_{ij}\chi_i(r), \tag{5}$$

where C_{ij} is the weighting coefficient and $\chi_i(r)$ is the symmetrized LCAO at the position r written as

$$\chi_i(r) = \sum (v,\, l,\, m)\, W^{il}_{vm}\varphi^{v}_{nlm}(r_v), \tag{6}$$

where v is the atom, l is the orbital quantum number, m is the magnetic quantum number, r_v is the coordinate referred to the atom v, W_{vm}^{il} is the symmetrization coefficient, and ϕ_{nlm}^{v} is the orbital function of atom v, which can be written as

$$\phi_{nlm}^{v}(r) = R_{nl}^{v}(r)Y_{lm}(r), \tag{7}$$

where $Y_{lm}(r)$ is taken to be the real spherical harmonics and $R_{nl}^{v}(r)$ is the radial part of the atomic orbital generated by numerical computation of the atomic problem. In this calculation, the electronic structure calculation shows the energy levels, PDOS, bond overlap population, atom contour maps, bond order, and net charge by Mulliken's population analysis [14]. The energy levels and PDOS are analyzed to obtain the energy gap and Fermi energy values for evaluating the electrical conductivity and Seebeck coefficient values.

II-2. Electrical conductivity determination

The electrical conductivity in an ionic crystal is given by

$$\sigma = Ne\mu, \tag{8}$$

where N is the number of ions (electrons and holes) per unit volume, e is the electron change and μ is the electron mobility. N can be written as

$$N = N_e + N_h = \frac{1}{4}\left(\frac{2mk_BT}{\pi\hbar^2}\right)^{3/2}\left(\frac{m^*}{m}\right)^{3/2}\exp\left[-\left(\frac{E_g}{2k_BT}\right)\right], \tag{9}$$

and $\mu = \mu_e + \mu_h = \frac{De}{k_BT}$, $D = \frac{1}{2}L_0\left(\frac{3k_BT}{m}\right)^{1/2}$; thus

$$\mu = \frac{1}{2}L_0\frac{e}{k_BT}\left(\frac{3k_BT}{m}\right)^{1/2}, \tag{10}$$

where N_e and N_h are the number of electrons and holes per unit volume, respectively; m is the mass; m^* is the effective mass of the ions; k_B is the Boltzmann constant (8.617 332 4(78) $\times 10^{-5}$ eVK^{-1}); D is the diffusion coefficient, which can be defined from the electron mean free path (L_0); E_g is the energy gap, which can be determined from the energy level; T is the temperature; $\hbar$ is the reduced Planck constant (6.582 119 28(15) $\times 10^{-16}$ eV.s); and μ_e and μ_h are the electron and hole mobilities, respectively. Combining Eq. (9) and (10) in (8), we can determine

$$\sigma = \frac{1}{8}\left(\frac{2mk_BT}{\pi\hbar^2}\right)^{3/2}\left(\frac{m^*}{m}\right)^{3/2}\frac{e^2}{k_BT}L_0\left(\frac{3k_BT}{m}\right)^{1/2}F, \tag{11}$$

where F is the $\exp\left[-\left(\frac{E_g}{2k_BT}\right)\right]$ term. From Eq. (11) when consider the density of states, $DOS\,(E)$, which is defined as

$$DOS\,(E) = \frac{V}{4\pi^2}\left(\frac{2m}{\hbar^2}\right)^{3/2}E^{1/2}, \tag{12}$$

where E is the energy; thus Eq. (11) can be expressed as

$$\begin{aligned}\sigma &= \frac{\pi^2 e^2}{2Vk_BT}L_0\left(\frac{1}{\pi}\right)^{3/2}\left(\frac{m^*}{m}\right)^{3/2}(k_BT)^2\left(\frac{3}{mE}\right)^{1/2}DOS\left(E\right)F \\ &= \frac{\pi^2 e^2}{2V}L_0\left(\frac{1}{\pi}\right)^{3/2}\left(\frac{m^*}{m}\right)^{3/2}k_BT\left(\frac{3}{mE}\right)^{1/2}DOS\left(E\right)F \\ &= \frac{\pi^2 e^2 k_BT}{2Vm}L_0\left(\frac{1}{\pi}\right)^{3/2}(m^*)^{3/2}\left(\frac{3}{mE}\right)^{1/2}DOS\left(E\right)F. \end{aligned} \tag{13}$$

When the term $m^* = \hbar^2\left(\frac{d^2E}{dk^2}\right)^{-1}$ and $E = \frac{\hbar^2}{2m}k^2$ then

$$m^* = \hbar^2\left(\frac{\hbar^2}{m}\right)^{-1}. \tag{14}$$

Consequently Eq. (13) is given by

$$\begin{aligned}\sigma &= \frac{\pi^2 e^2 k_BT}{2Vm}L_0\left(\frac{1}{\pi}\right)^{3/2}\left(\hbar^2\left(\frac{\hbar^2}{m}\right)^{-1}\right)^{3/2}\left(\frac{3}{mE}\right)^{1/2}DOS\left(E\right)F \\ &= \frac{\pi^2 e^2\hbar^3 k_BT}{2m}L_0\left(\frac{1}{V}\left(\frac{m}{\pi\hbar^2}\right)^{3/2}\left(\frac{3}{E}\right)^{1/2}\right)DOS\left(E\right)F. \end{aligned} \tag{15}$$

From Eq. (12), (15) can be written as

$$\sigma = \frac{2\pi^2 e^2\hbar^3}{3m^2}L_0 DOS^2\left(E\right)k_BT\exp\left[-\left(\frac{E_g}{2k_BT}\right)\right]. \tag{16}$$

From the Fermi-Dirac distribution function, $f(E) = \frac{1}{\exp\left[\frac{(E-E_F)}{k_BT}\right]+1}$, $f(E) = \frac{1}{\exp\left[\frac{(E-E_F)}{k_BT}\right]+1}$. The significance of Fermi energy is most clearly seem by setting $T = 0$ K, the probability is equal 1 for energies less than the Fermi energy and zero for energies greater than the Fermi energy [15, 16] so that Eq. (16) is given by

$$\sigma = \frac{2\pi^2 e^2\hbar^3}{3m^2}L_0 DOS^2\left(E_F\right)\exp\left[-\left(\frac{E_g}{2k_BT}\right)\right], \tag{17}$$

where $DOS\left(E_F\right)$ is the density of states at the Fermi level. The relationship between the electrical conductivity and temperature of the semiconductor is given by [15, 16]

$$\sigma(T) \approx \sigma_0\exp\left(-\frac{E_g}{2k_BT}\right), \tag{18}$$

where σ_0 is the minimum metallic conductivity at $T = 0$ K. σ_0 is determined by the scattering of electrons by phonons at high temperature using Mott's equations [16]:

$$\sigma_0 \approx \frac{2\pi e^2\hbar^3}{3m^2}L_0\left\{DOS(E_F)\right\}^2, \tag{19}$$

where L_0 is estimated from the lattice parameter a (4.264 Å) and $DOS(E_F)$ is determined from the molecular orbital calculations at the Fermi level.

II-3. Seebeck coefficient determinations

The Seebeck coefficient is evaluated via the Fermi energy. The Fermi energy of a semiconductor is one half of E_g; from the Fermi-Dirac distribution the Seebeck coefficient can be expressed as follows [17]:

$$S(T) = \frac{k_B}{e} \ln[(1 - f(E))/f(E))]. \tag{20}$$

Replacing the Fermi-Dirac distribution function to obtain the Seebeck coefficient,

$$S(T) = \frac{k_B}{e} \left[\frac{(E - E_F)}{k_B T} \right]. \tag{21}$$

When $(E - E_F) \approx E_F$ at $T = 0$ K, so that Eq. (21) is given by

$$S \approx \left(\frac{k_B}{e} \right) \left(\frac{E_g}{2k_B T} \right) \approx \left[\frac{E_g}{2eT} \right]. \tag{22}$$

III. CALCULATION OF THE FIRST PRINCIPLES MOLECULAR ORBITAL METHOD

The steps of the computational detail of the calculation method are shown more carefully by Seetawan *et al.* [18], for which we used the dvscat code [10]. In Table I the calculation of the electronic structures of Sb_2Te_3 was performed with the designed cluster model by using the ordinary data of the crystal structure of Sb_2Te_3 [19].

TABLE I: The crystallography data of Sb_2Te_3 [19].

Space group	Lattice parameter	Atom	X	Y	Z
166	$a = 4.264$	Te (1)	0	0	0
R-3m	$c = 30.458$ Å	Sb	0	0	0.398
		Te (2)	0	0	0.787

The Te and Sb atoms are generated randomly for placing into the unit cell. The cluster model is designed by deleting atoms based on a unit cell and then checking the symmetry of the cluster model. The matrix elements of the Hamiltonian and overlap integrals are evaluated as weight sums of the integrand values at discrete sample points instead of the conventional integration procedure [10, 20]. The number of the sample points is 17,000. The computer calculation was carried out using a personal computer which consists of an AMD sempron of 2.45 GHz, with an 850 chipset and 2.00 GB, DDR2.

IV. RESULTS AND DISCUSSION

IV-1. Electronic structure

In Figure 1 (a)–(c), the $Sb_{12}Te_{22}$ cluster model is employed for 1/3 of the hexagonal structured unit cell. The cluster model consists of 12 Sb atoms and 22 Te atoms, and high symmetry are compared the report of L. Xuelai *et al.* [9].

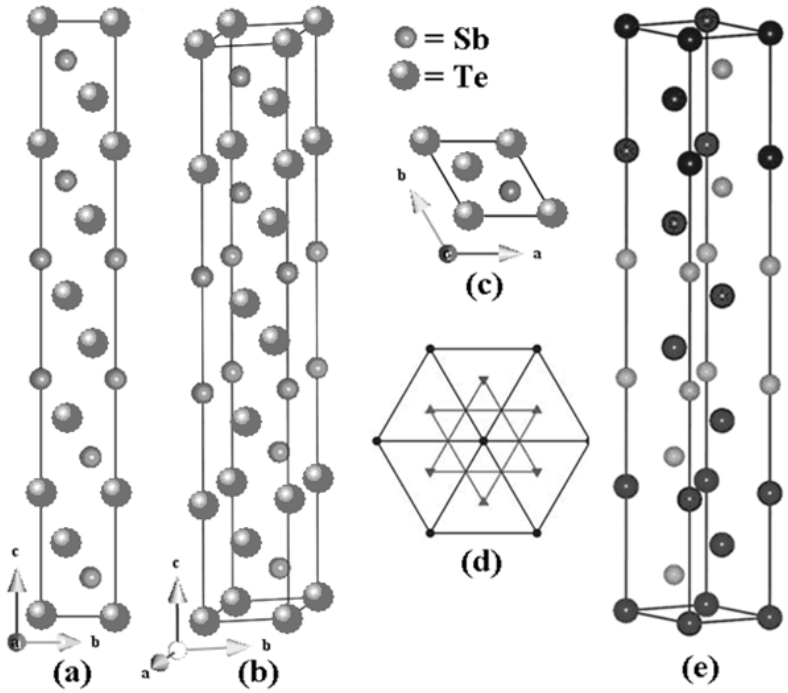

FIG. 1: $Sb_{12}Te_{22}$ cluster model calculation in the plane (a) (100), (b) (100) rotated by 45°, (c) 001, (d) Sb_2Te_3 crystal structure symmetry, and (e) Sb_2Te_3 crystal structure [9], in which the Sb and Te atoms are (green) small and (blue) large, respectively.

The radial atomic orbital wave functions of Sb and Te are obtained as the Sb4d, 5s and 5p and Te4d, 5s and 5p orbitals corresponding to the Sb_2Te_3 crystal structure, as shown in Figure 2. The energy level and the density of states of the $Sb_{12}Te_{22}$ cluster model can be evaluated in the next step.

In Figure 3, the total energy level is shown including the conduction band (dot lines) and valence band (solid lines) together with the partial orbitals. The partial orbital energy level of the $Sb_{12}Te_{22}$ cluster model is related to the density of states. The energy gap is determined by the difference of the lowest unoccupied molecular orbital (LUMO) at wave function number 879 and the highest occupied molecular orbital (HOMO) at wave function number 878, as shown in Figure 4. The direct energy gap [21] of $Sb_{12}Te_{22}$ of the cluster model is about 0.152 eV, which agrees well with Jariwala *et al.* [6].

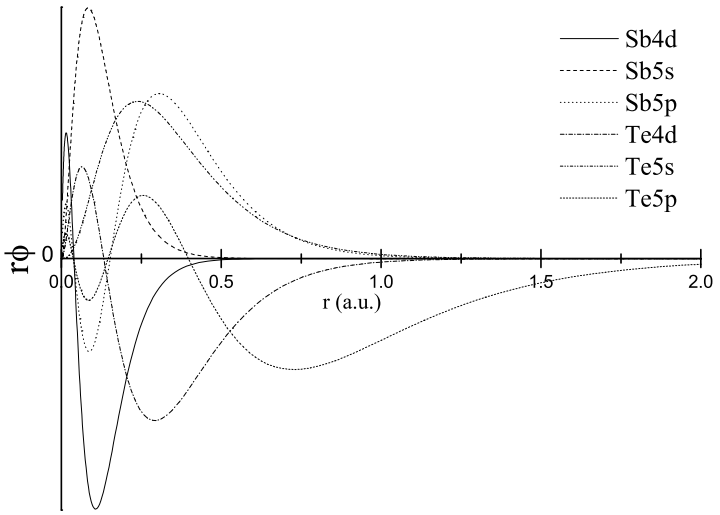

FIG. 2: Radial functions of the Sb4d, 5s and 5p and Te4d, 5s and 5p orbitals.

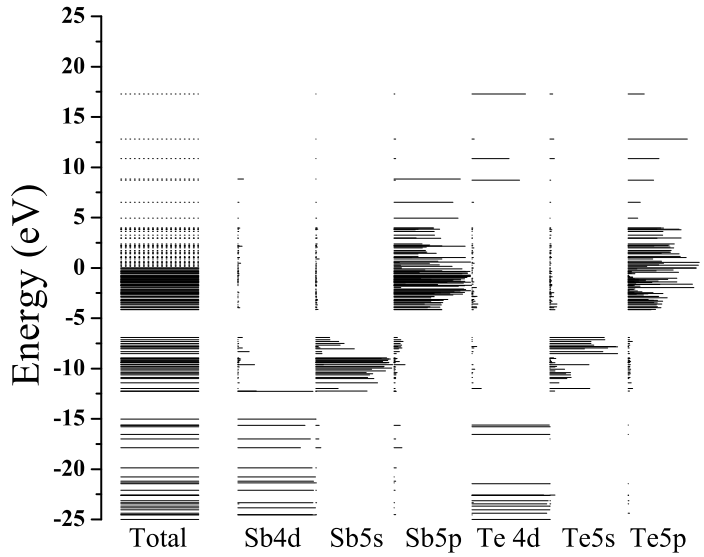

FIG. 3: The energy level diagram of the $Sb_{12}Te_{22}$ cluster model composed of the total, Sb4d, Sb5s, Sb5p, Te4d, Te5s, and Te5p.

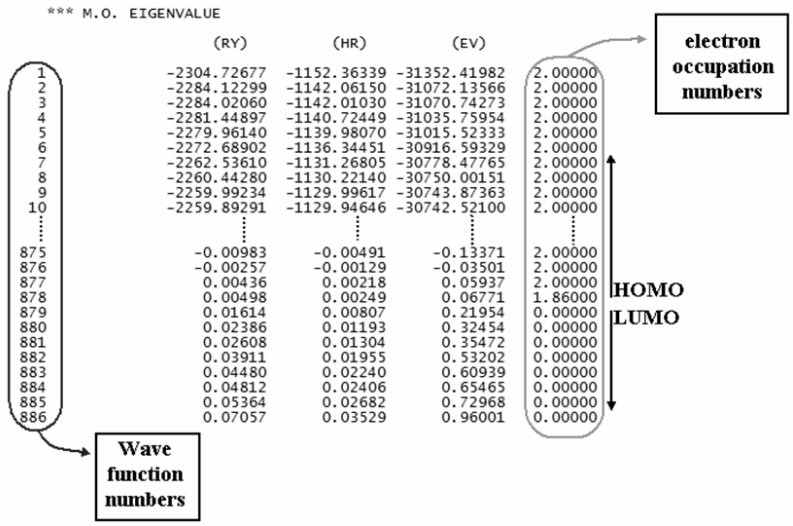

FIG. 4: MO eigenvalues of the $Sb_{12}Te_{22}$ cluster model at the HOMO and LUMO position.

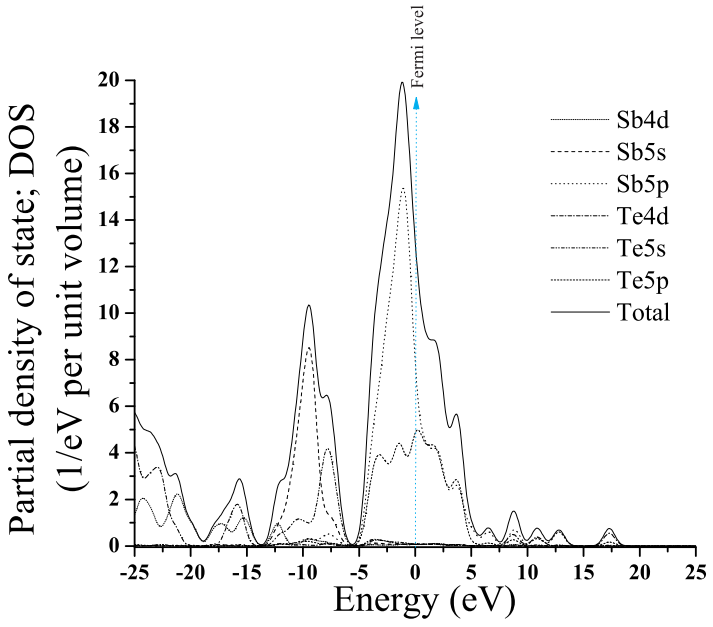

FIG. 5: The partial density of state of the $Sb_{12}Te_{22}$ cluster model.

Figure 5, the partial density of state of the $Sb_{12}Te_{22}$ cluster model composed the total Sb4d, Sb5s, Sb5p, Te4d, Te4s and Te5p, which the total density of state was nearly

Fermi level affected by Te5p and Sb5p orbitals because their used the ionic of Sb^{+3} and Te^{-2} indicate the metallic behavior.

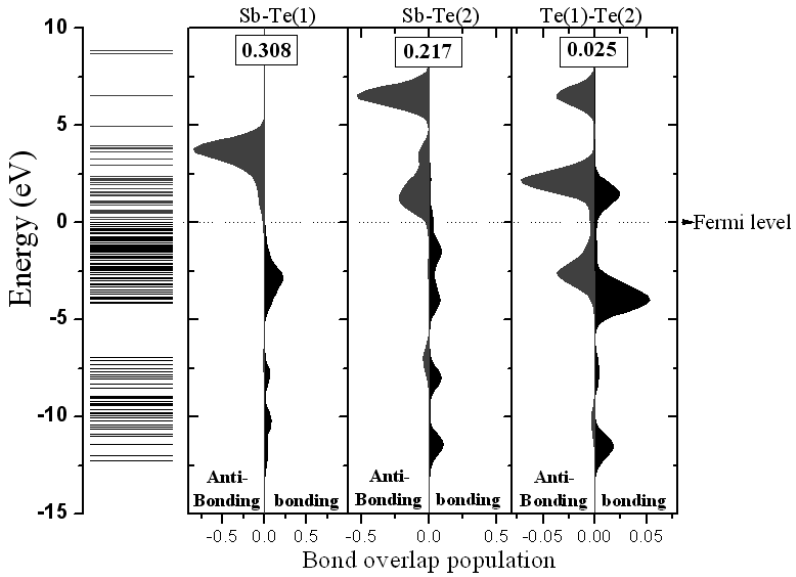

FIG. 6: The energy level diagram and bond overlap population diagram of Sb-Te(1) Sb-Te(2) and Te(1)-Te(2).

Figure 6, the bond overlap population diagram shows the bonding and anti-bonding of Sb-Te(1), Sb-Te(2), and Te(1)-Te(2) and indicates that the Sb-Te interaction arises mainly from the Sb5p and Te5p hybridization. The bond order is obtained by the difference between the bonding and anti-bonding. The bond length and bond order of Sb-Te(1), Sb-Te(2), and Te(1)-Te(2) are 3.0655 Å, 0.308; 3.2579 Å, 0.217; and 4.264 Å, 0.025, respectively. These bonds indicate the strength of the covalent bonding.

The atomic contour map in the plane (a) 100 and 001, and (b) a bird's-eye view of the atom in the plane 100 and 001 as shown in Figure 7.

IV-2. Electrical conductivity

The electrical conductivity of the $Sb_{12}Te_{22}$ cluster model is shown in Figure 8, together with that of Chen *et al.* [22] and Yu *et al.* [23] in the same temperature range. The electrical conductivity is 0.59×10^4 Sm^{-1} using Eq. (18) at 300 K. The electrical conductivity increases with increasing temperature in the range 300–700 K.

IV-3. Seebeck coefficient

The Seebeck coefficient of the $Sb_{12}Te_{22}$ cluster model is shown in Figure 9, together with that of Gu [24] in the same temperature range. The Seebeck coefficient value is 253 μVK^{-1} at 300 K and is decreasing with increasing temperature in the range 300–700 K.

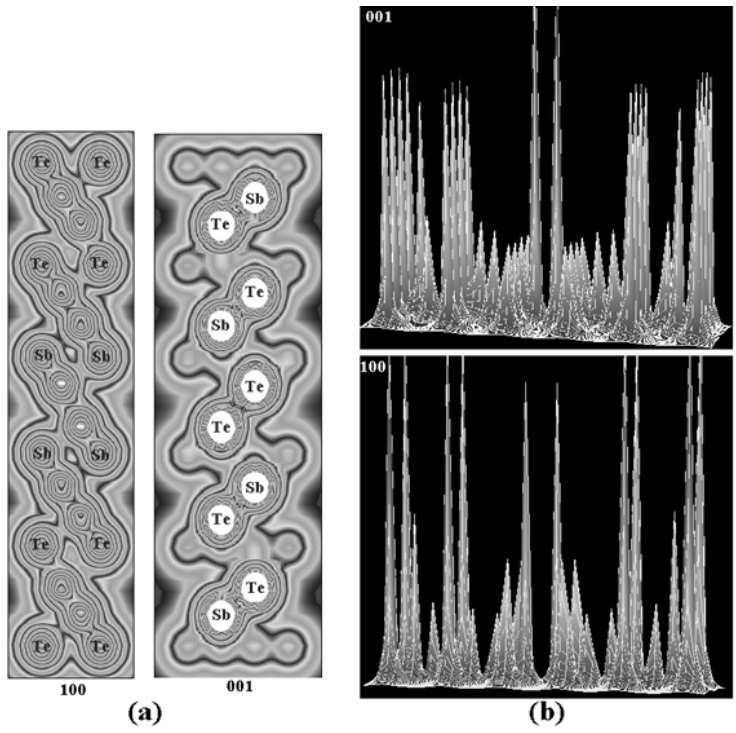

FIG. 7: The atomic contour map in the plane (a) 100 and 001, and (b) a bird's-eye view of the atom in the plane 100 and 001.

V. CONCLUSION

The electronic structure of Sb_2Te_3 was calculated by the molecular orbital method for the predication of TE properties. The $Sb_{12}Te_{22}$ cluster model is shown as 1/3 unit of the hexagonal structured unit cell for Sb_2Te_3. The direct energy gap of the $Sb_{12}Te_{22}$ cluster model is about 0.152 eV, and the density of states at the Fermi level is affected by the Te5p and Sb5p orbitals indicating metallic behavior. The electrical conductivity and Seebeck coefficient agreed with the literature data at the same temperature range.

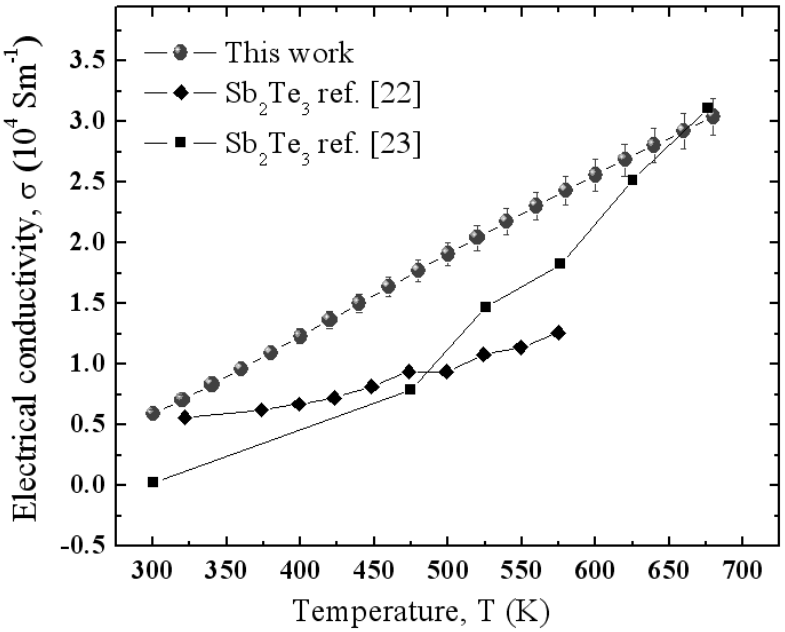

FIG. 8: The electrical conductivity of the $Sb_{12}Te_{22}$ cluster model.

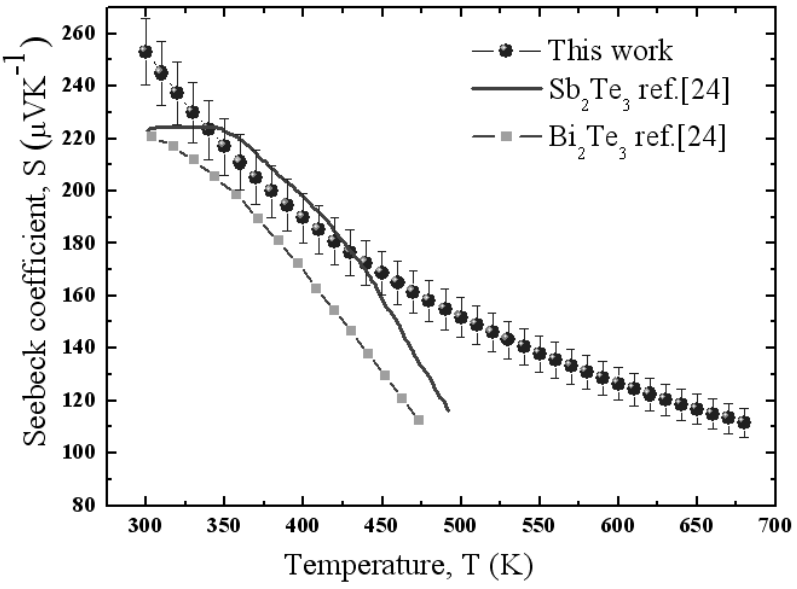

FIG. 9: The Seebeck coefficient of the $Sb_{12}Te_{22}$ cluster model.

Acknowledgements

The financial support from Thailand Graduate Institute of Science and Technology, NSTDA (TGIST: TG-33-99-52-037M) is gratefully acknowledged.

References

[1] T. Thonhauser, G. S. Jeon, G. D. Mahan, and J. O. Sofo, Phys. Rev. B **68**, 205207 (2003).
[2] H. Zhang *et al.*, Nature **5**, 438 (2009).
[3] R. Venkatasubramanian, E. Siivola, and T. Colpitts, Nature **413**, 597 (2001).
[4] R. Zhang *et al.*, Solid State Sci. **12**, 1168 (2010).
[5] G. A. Thomas *et al.*, Phys. Rev. B **46**, 1553 (1992).
[6] B. Jariwala and D. V. Shah, J. Cryst. Growth. **318**, 1179 (2011).
[7] I. Y. Erdogan and U. Demir, J. Electro. Anal. Chem. **633**, 253 (2009).
[8] V. A. Kul'bachinski, H. Ozaki, Y. Miyahara, and K. Funagai, J. Exp. Theor. Phys. Lett. **97**, 1212 (2003).
[9] L. Xuelai *et al.*, Solid State Sci. **13**, 131–134 (2011).
[10] E. D. Ellis and G. S. Painter, Phys. Rev. B **82**, 2887 (1970).
[11] H. Adachi, M. Tsukada, and C. Satoko, J. Phys. Soc. Jpn. **45**, 875 (1978).
[12] J. C. Slater, *Quantum Theory of Molecules and Solids*, (The Self-Consistent Field for Molecules and Solids, Vol. 4) (McGraw-Hill, New York, 1974). Chap. 1.
[13] K. Kushida, Y. Ichihashi, Y. Suzuki, and K. Kuriyama, Phys. B **405**, 2305 (2010).
[14] R. S. Mulliken, J. Chem. Phys. **23**, 1833 (1955).
[15] V. Sklyarchuk, Y. Plevachuk, S. Mudry, I. Shtablavyi, and B. Sokolovskii, J. Phys.: Conf. Seri. **98**, 062003 (2008).
[16] N. F. Mott and E. A. Davis, *Electron Processes in Non-Crystalline Materials*, (Clarendon Oxford, 1979). Chap. 6, University Press, 1st ed. 1971, 2nd ed. 1978.
[17] N. F. Mott, E. A. Davis, and R. A. Street, Philos. Mag. **32**, 961 (1975).
[18] T. Seetawan, A. Vora-Ud, P. Chainaronk, C. Thanachayanont, and V. Amornkitbamrung, Comp. Mater. Sci. **49**, S225 (2010).
[19] P. Villars and L. D. Calvert, *Pearson's Handbook of Crystallographic Data for Intermetallic Phases* (In_3PSe_3-Zr, V. 4), 2nd ed. (ASM International, 1996) p. 5195.
[20] F. W. Averill and D. E. Ellis, J. Chem. Phys. **59**, 6412 (1973).
[21] J. W. Park *et al.*, Appl. Phys. Lett. **93**, 021914 (2008).
[22] J. Chen *et al.*, Chem. Mater. **22**, 3086 (2010).
[23] J. Yu *et al.*, Appl. Sur. Sci. **253**, 6125 (2007).
[24] Q. Gu, arXiv:1101.2487v2 [cond-mat.mtrl-sci] 27 Jan 2011.